Journal Name

COMMUNICATION

4-Pyridylisocyanide Gold(I) and Gold(I)-plus-Silver(I) Luminescent and Mechanochromic Materials: The Silver Role

Verónica Conejo-Rodríguez,[a] Marconi N. Peñas-Defrutos,[a] and Pablo Espinet[a,*]

Received 00th January 20xx,

Accepted 00th January 20xx

DOI: 10.1039/x0xx00000x

www.rsc.org/

Crystallographic and DFT examination of the metalloligands [AuAr(CNPy-4)] (Ar = C_6F_5 (1), $C_6F_3Cl_2$-3,5 (2)) and their silver complexes [Ag[AuAr(CNPy-4)]$_2$](BF$_4$) (3 and 4) support that the marked luminescence red-shifts observed on moving from 1 to 2, from 1,2 to 3,4, or upon grinding, are not caused by electronic differences (either by changing the aryls C_6F_5/$C_6F_3Cl_2$, or by N coordination to silver), nor by non-existent Au···Ag interactions. They are always due to structural changes disturbing stronger π-π stackings in order to allow for shorter Au···Au interactions.

Many gold(I) organometallic compounds are luminescent and show mechanoresponsive luminescence.[1] Of specific interest for this work are some recent papers by Ito and others, reporting that aryl or fluoroaryl gold(I) isocyanide complexes display luminescent mechanochromism.[2-4] This refers to changes in luminescence associated to crystal-to-crystal or crystal-to-amorphous phase transitions, either produced by mechanical stress or by recrystallization; solvent uptake or release is sometimes involved in the last case. These structural changes affect the formation, breaking, or strength of Au···Au interactions. As an example, the homobimetallic pentafluorophenyl complex in Fig. 1, which does not display aurophilic interactions in its original single crystal X-ray structure, changes its luminescence upon grinding.[2]

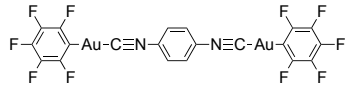

Figure 1.

4-Pyridylisocyanide (CNPy-4) can act as bidentate ligand and their two different coordinating functions are good to bind Au^{I}/Ag^{I} selectively. We decided to use it to prepare [AuAr(CNPy-4)] complexes (Ar = C_6F_5 = Pf (**1**); Ar = $C_6F_3Cl_2$-3,5 = Rf, (**2**)) and [Ag[AuAr(CNPy-4)]$_2$](BF$_4$) (**3** and **4**),[5] to compare their photophysical properties and the possible effect of the presence of silver. It is well known that introducing a second metal centre (M) on gold complexes often produces materials with direct Au···M interactions that have dramatic effects on the luminescence.[6,7] Even if this were not the case, we might expect differences in the photophysical properties of **1**-**4**, either due to the different electronegativity of the aryls Pf and Rf, or induced upon N-coordination of the metalloligands [AuAr(CNPy-4)] to silver.

The syntheses of **1**,**2** were carried out by ligand substitution of tht (tetrahydrothiophene) on the corresponding [AuAr(tht)] complex.[8] The 2:1 reactions of **1** or **2** with AgBF$_4$ in acetone led to **3**,**4** (Eqn. 1). The complexes where fully characterized by C,H,N analyses, IR, ^{1}H and ^{19}F NMR, and single-crystal X-ray diffraction when feasible crystals could be obtained (see ESI).

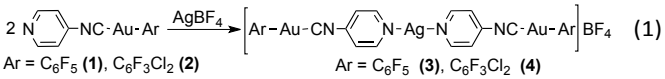

Ar = C_6F_5 (**1**), $C_6F_3Cl_2$ (**2**) Ar = C_6F_5 (**3**), $C_6F_3Cl_2$ (**4**) (1)

The ligand and the complexes display absorption bands in the UV-Vis spectra in the range 200-300 nm in dichloromethane solution, with large extinction coefficients of 10^4 M^{-1} cm^{-1}. These are typical, in other cases studied, of a mixture of π-π^* transitions based on the pyridyl rings, and Au-π^* *or* π-π^* transitions in the fluorinated aryl.[7] Interestingly the four UV-Vis spectra of **1**-**4** are almost superimposable (Fig. ESI21). This means that in the individual molecules the electronegativity difference between Pf and Rf, as well as the electronic polarization upon N-coordination to silver, are almost negligible.

Neither the ligand nor the complexes display luminescence in solution. However, in the solid state they show interesting behaviour and remarkable differences that should necessarily be assigned to structural changes in the crystals of **1**-**4**.

[a] *IU CINQUIMA/Química Inorgánica, Facultad de Ciencias, Universidad de Valladolid, 47071-Valladolid, Spain. E-mail: espinet@qi.uva.es*

Electronic Supplementary Information (ESI) available: [Synthesis and full characterisation of the complexes, X-ray and computational details; 27 pages]. See DOI: 10.1039/x0xx00000x

Single crystal X-ray studies could be made for complexes **1**, **2** and **4**, which show structures where Au···Au interactions and π-π stacking interactions can be identified. The crystal of complex **1** was obtained by slow diffusion of n-hexane into a solution of **1** in dichloromethane. The X-ray structure (Figure 2) shows a parallel infinite arrangement of the molecules with Pf-Pf and py-py stacking, and Au···Au long distance (3.817 Å). The Pf and py rings are not coplanar, but make a dihedral angle of 31.5°.

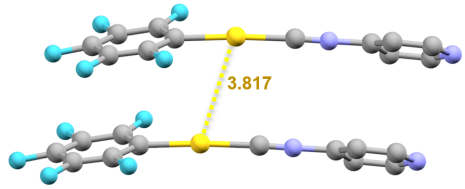

Figure 2. Crystal structure of **1**. Distance in Å

Different mixtures of two polymorphs of compound **2** were obtained depending on the crystallization conditions. By slow diffusion of n-hexane into a solution of **2** in dichloromethane needle-shaped crystal were predominant. The X-ray of one of them corresponds to the structure in Figure 3, and is named **2α**. In a faster procedure consisting of evaporation from a dichloromethane/n-hexane solution, plate-like crystals of polymorph **2β** were predominant. The powder X-ray diffraction (PXRD) pattern of the bulk product **2** contains mostly the peaks expected from the single crystal structures **2α** and **2β** (Figure ESI20).[9] This mixture of polymorphs is also observed in the luminescent properties of **2**, as discussed later. The crystal of **2α** contains pairs of two kinds of molecules (**2a** and **2b** in 1:1 ratio), as shown in Fig. 3. They differ in the dihedral angle between the Rf and the Py planes, which are almost coplanar (dihedral angle 3°) in the pair **2a**, and make a 41° angle in the pair **2b**.

The **2a** molecules are associated in the crystal as antiparallel pairs, and show within the pair one Au···Au interaction, at 3.315 Å, and Rf-py π-π stacking interactions at 3.446 Å. The pair of **2b** molecules is defined by the existence of inter-halogen C–F_{ortho}···Cl_{meta}–C contacts within each pair, with distance d(F···Cl) = 3.025 Å (the sum of vdW radii is 3.1–3.9 Å),[10] and does not have aurophilic interactions. Furthermore, a shorter contact (d(F···Cl) = 2.998 Å) is found between **2a** and another neighbouring **2b** (not shown in Fig. 3, see Fig. ESI15).[11,12] Additionally, the pair **2b** has π-π Rf-Rf stacking (at 3.580 Å), and π-π Rf-py stacking (at 3.589 Å) with **2a**, while their own Py rings are tilted and do not participate in any stacking. A perhaps more expressive view of the packing is given in the space-fill representation in Figure 3.

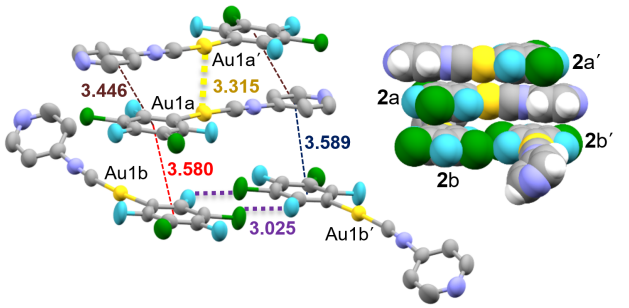

Figure 3. Two views of packing interactions in complex **2α**. Distances in Å.

The structure of **2β** (Figure ESI16) is more complicated (12 molecules in the asymmetric unit) and shows shorter Au···Au distances (3.2344(16) and 3.2768(16) Å) than **2α**. This is used later in the discussion.

Crystals of complex **4** were obtained by diffusion, in the dark at room temperature, of a solution of $AgBF_4$ in acetone layered on top of a solution of complex **2** in dichloromethane. After 24 h, orange crystals had been formed at the interphase of the two solvents. The structure contains only one kind of molecule in the asymmetric unit (Fig. 4, above), including half acetone of crystallization, and confirms the molecular proposal in Equation 1: the two N atoms of the two gold metallopyridine moieties linearly coordinate the silver centre. The BF_4^- anions are tightly attached to Ag^+, with the atoms at F–Ag vdW distances.

The packing arrangement of **4** (Fig. 4, below) consists of pairs of parallel molecules with π-π Rf-Rf stacking at 3.512 Å. Each Au centre of these molecular pairs makes fairly long Au···Au interactions at 3.472 Å, obviously impeded to be shorter by the neighbour π-π Rf-Rf stacking at 3.512 Å. These pairs are perpendicularly arranged to other identical pairs. In the perpendicular arrangement the π-π Rf-Rf stacking is lost, but much shorter Au···Au interactions at 3.137 Å are created.[13]

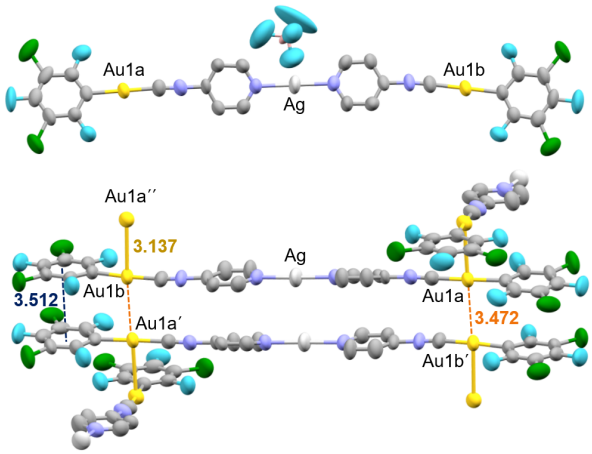

Figure 4. Above: asymmetric unit for complex **4**. Au1a and Au1b are crystallographically non-equivalent due to different dihedral angles between Rf and Py moieties. Below: four molecules showing the gold-gold and π-π stacking interactions (anions and acetone omitted for clarity). Distances in Å.

The $Ag_2(BF_4)_2$ moieties probably play three structural roles: *i)* The BF_4^- counteranions (omitted in Figure 4 below), are situated above and below the Ag---Ag (3.715 Å) line, each one closer to each respective Ag. This arrangement precludes Ag

involvement in Ag···Ag or Ag···Au interactions. *ii)* It also precludes stacking of the py rings, which make in fact dihedral angles of 16° suggesting no π-π dispersion in that molecular zone. *iii)* Probably another role of silver is that it connects two dipolar complexes in a trimetallic unit with no dipolar moment. In the absence of dipolar moment, the often preferred infinite antiparallel arrangement of dipolar molecules cannot be formed, and the system finds higher crystallographic stabilization in a crystal structure alternating perpendicular and parallel disposition of the molecules,[14,3,1a] which allows to achieve shorter Au···Au contacts at 3.137 Å between perpendicular molecules.

The ligand is not luminescent, but the emission spectra of **1**-**4** in solid state at room temperature display in all cases very strong bands (Figure 5). Moreover, **1** and **2** present clear mechanochromism with remarkable red-shift of the emissions.

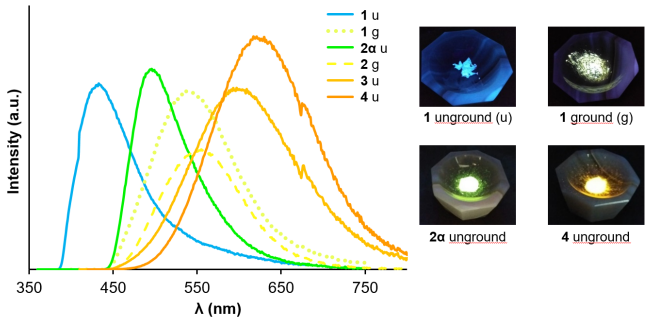

Figure. 5. Emission spectra of compounds **1**-**4** in the solid state, before and after grinding.

Table 1 collects the main parameters of the luminescence observed for unground and ground samples at room temperature and in glassy state at 77K.[15,16] According to the comments above, all the significant differences should find a structural justification.

Table 1. Excitation and emission data (nm) before and after grinding (solid state, 298 K), and in glassy state at 77K

Comp.[a]	λ_{exc}	λ_{emis}	Φ (%)	τ_{av} (ns)[c]	d(Au···Au)
1 (u)	343	434	21.0	9.65	3.82 (Å)
1 (g)	390[b]	540	18.0	677	-
1 (glassy)	401	575		712	
2α (u)	343,[b] 387	497	9.9	267	3.32 (Å)
2β (u)	343, 387[b]	523			3.23 (Å)[d]
2 (g)	397	557	15.9	488	-
2 (glassy)	391	557		793	
3 (u)	387	600	2.4	441	-
3 (g)	399	580	5.2	467	-
4 (u)	387	623	42.0	326	3.14 (Å)
4 (g)	387	620	52.0	388	-

[a] Unground (u) or ground (g). [b] Most intense peak.. [c] $\tau_{av} = (A_1\tau_1^2 + A_2\tau_2^2 + \cdots)/(A_1\tau_1 + A_2\tau_2 + \cdots)$. [d] Shortest distance

Comparing the emission spectra of unground **1** and **2α**, under UV-irradiation complex **1** exhibits blue emission at 434 nm, while complex **2α** exhibits pale green emission at 497 nm. The structure of [AuPf(CNPy-4)] (**1**) shows that all the aromatic rings are involved in π-π Pf-Pf and py-py stacking, and the Au···Au distance is very long (3.817 Å). In contrast, the short F···Cl contacts found in the structure of **2α** seem to be strong enough to induce a different crystal structure, overall less efficient for π-π stacking (half of the Py rings are not involved in stacking), but containing significantly shorter Au···Au distances (3.315 Å) than in **1**, for half or the gold atoms. Thus the emission red-shift (2920 cm^{-1}) from **1** to **2α**, although associated to the change fluorinated aryl (Pf vs. Rf), is not due to electronic differences between them but to a structural change leading to shorter Au···Au distances in **2α**. Comparing **2α** and **2β**, the latter, with some shorter Au···Au distances shows, consistently, a slightly red-shifted emission (1000 cm^{-1}).

As for the mechanochromism, upon grinding [AuPf(CNPy-4)] (**1**) in an agate mortar, the blue luminescence of **1** changes to an intense yellow luminescence (Figure 5), corresponding to a red-shift of 4520 cm^{-1}. For the green luminescent [AuRf(CNPy-4)] (**2α**) grinding produces a smaller red-shift (2170 cm^{-1}), but a yellow luminescence almost coincident with ground **1** (they differ in 565 cm^{-1}). This supports that **1** and **2α** lose crystalline order upon grinding (detected in the PXRD patterns, Fig. ESI16),[17] and the significantly different structures and Au···Au distances in the two unground solids converge to almost identical structures with shorter Au···Au interactions in the ground samples, which are responsible for the very high red-shift observed. The emission spectra in the in glassy matrix in dichloromethane at 77 K are close to those in the ground material of **1** and **2** (details in ESI).

Upon coordination of **1** or **2** to silver(I), a large red-shift is observed in $[Ag[AuAr(CNPy\text{-}4)]_2](BF_4)$ (**3** and **4**) (6370 cm^{-1} shift for **3** and 4070 cm^{-1} for **4**), leading **3**,**4** to display infrequent orange luminescence at very close wavelengths (600 (**3**) and 623 (**4**) nm, respectively).[3,18] This proximity of wavelengths suggests that **3** shares, with minor variations, the structure found for **4** (Figure 4). As mentioned above, this structure discards Au···Ag contacts as the cause of the red-shift observed for **3** and **4** compared to **1** and **2**.

The structure of **4** with very short (3.137 Å) Au···Au distances in the single crystal, explains that a large shortening and modification of the emission wavenumber upon grinding cannot be expected. Complex **4** shows the highest quantum yield of the series, whether unground (42%) or ground (52%).

Red-shift effects have been observed and theoretically studied in many cases of aurophilic interactions at short distances.[3,14,20] In order to explain the large red-shift upon formation of **4** from **2α** (the case of **3** from **1** is similar), a TD-DFT study (wb97xd level) was carried out on a representative crystallographic fragment (6 units of [AuRf(CNPy-4)] in both cases), imposing the arrangement and distances observed in the X-ray studies of **2α** and **4**. The exclusion of Ag in the selection of the fragment for **4** is obliged because it is not possible to take a part of made of the X-ray structure of full molecules that constitutes a symmetric fragment. This imposed sacrifice of the $AgBF_4$ link may look a serious problem, but luckily the electronic effect on the orbitals involved in

electronic transitions is probably small considering that the four UV-Vis spectra of **1**-**4** are almost superimposable. Further support to this is the calculations for molecule **4** in Figure 6, which show that there is no participation of Ag in the frontier orbitals supposedly involved in the emission. Of course some indirect influences on the energies of these orbitals in the real crystal cannot be excluded, but the fact is that utilization of this crystallographic fragment provides qualitatively satisfactory results, as discussed below.

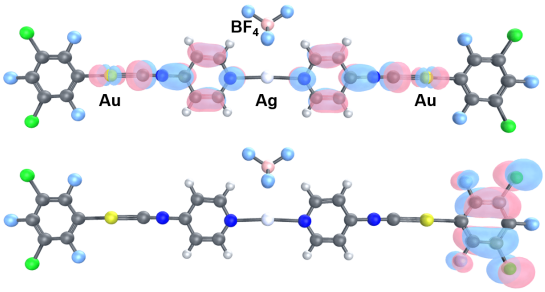

Figure 6. HOMO (below) and LUMO (above) orbitals of molecule **4**.

Figure 7 illustrates the origin of the green to orange red-shift observed from **2α** to **4**. First of all, the DFT calculations show that there is an important change in gold participation (8% *vs.* 79% respectively, more details in Table ESI8) comparing HOMO (2), and σ*-HOMO (4). Consequently, the energy of σ*-HOMO (4) is is much more sensitive to the Au···Au distance than that of HOMO (2), and suffers a higher destabilization at shorter distances. In contrast, the LUMOs of **2α** and **4** are both mostly based on the isocyanide ligand (83% for LUMO (2) and 76% for LUMO (4)), and their energies must be much less sensitive to the Au···Au distance.[19] The balance of these variations is a considerably decrease of the HOMO/LUMO energy gap for **4**, with short Au···Au distance, compared to **2α**, with large Au···Au distance, and consequently a remarkable red-shift in **4** compared to **2α**. For the reasons discussed above, the singlet excitation energies calculated by TD-DFT for these small-size fragments (4.60 eV = 269 nm for **2**; 3.56 eV = 348 nm for **4**) reflect only qualitatively the red-shift experimentally observed upon coordination to silver (497 nm for **2α**; 623 nm for **4**).

In conclusion, the luminescence changes observed by participation of Ag (**1**,**2** *vs*. **3**,**4**) are not due to a silver effect of intra-molecular electron polarization upon coordination to Ag, which is small, but to the symmetric nature of the Ag complex formed and to the steric effects of the Ag(BF_4) moiety. Similarly, the variations observed for **1** vs. **2** are not due to the electronegativity difference between Pf and Rf but to structural differences depending in this case on the absence or presence of inter-halogen interactions. Thus in all cases studied here the observed red-shifts comparing **1** vs. **2**, **1**,**2** *vs*. **3**,**4**, or unground *vs*. ground samples, are associated to structural modifications, promoted by different phenomena but all having in common that they disturb the initial structures based in good Ar-py, py-py, or Ar-Ar π-π stacking and lead to alternative crystallographic arrangements with shorter Au···Au interactions.

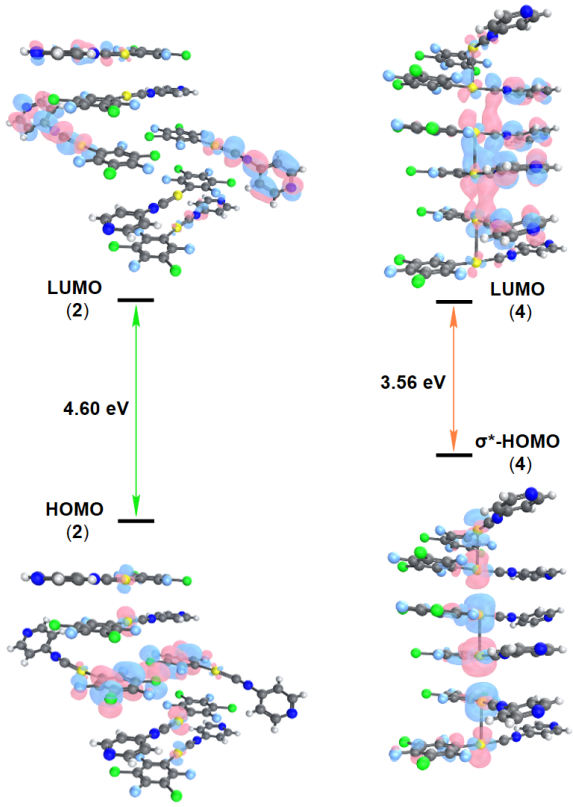

Figure 7. HOMO-LUMO[19] orbitals and TD-DFT excitation energies for selected fragments of **2α** and **4**.[19] Single point calculations are made based on the X-Ray structures (Figures 3-4). The identical positioning of LUMO (2) and LUMO (4) is arbitrary. It is meant to graphically highlight in a simple image the transition energy difference for complexes **2α** and **4**.

We thank the Spanish MINECO (Project CTQ2017-89217-P) and the Consejería de Educación of the Junta de Castilla y León (Project VA038G18) for financial support, the MINECO for a FPI grant to V. C.-R., and the Spanish MECD for a FPU grant to M. N. P.-D. Help of Dr. Jose M. Martin-Alvarez and an anonymous referee in the solution of the structure of **2β**, and of Dr. Max García-Melchor in the application DFT to these systems, is also gratefully acknowledged.

Conflicts of interest

There are no conflicts to declare.

Notes and references

1 (a) Y. Sagara, S. Yamane, M. Mitani, C. Weder and T. Kato, *Adv. Mater.*, 2016, ***28***, 1073–1095. (b) P. Xue, J. Ding, P. Wang and R. Lu, *J. Mater. Chem. C*, 2016, ***4***, 6688—6706. (c) J. M. López-de-Luzuriaga, M. Monge and M. E. Olmos, *Dalton Trans.*, 2017, ***46***, 2046–2067. (d) C. Jobbágy and A. Deák, *Eur. J. Inorg. Chem.*, 2014, 4434–4449. (e) V. W.-W. Yam, V. K.-M. Au and S. Y.-L. Leung, *Chem. Rev.*, 2015, ***115***, 7589–7728.

2 H. Ito, T. Saito, N. Oshima, N. Kitamura, S. Ishizaka, Y. Hinatsu, M. Wakeshima, M. Kato, K. Tsuge and M. Sawamura, *J. Am. Chem. Soc.* 2008, ***130***, 10044–10045.

3 T. Seki, Y. Takamatsu and H. Ito, *J. Am. Chem. Soc*., 2016, ***138***, 6252−6260.

4 For other examples of [AuR(CNAr)] (R = aryl, haloaryl) mechanochromic compounds see: (a) T. Seki, K. Sakurada and H. Ito, *Chem. Commun*., 2015, ***51***, 13933–13936. (b) T. Seki, T. Ozaki, T. Okura, K. Asakura, A. Sakon, H. Uekusa and H. Ito, *Chem. Sci*., 2015, ***6***, 2187–2195. (c) J. Liang, F. Hu, X. Lv, Z. Chen, Z. Chen, J. Yin, G.-A. Yu and S. H. Liu, *Dyes Pigm*., 2012, ***95***, 485–490. (d) M.-J. Wang, Z.-Y. Wang, P. Luo, B. Li, L.-Y. Wang and S.-Q. Zang, *Cryst. Growth Des.*, 2019, ***19***, 538–542. (e) J. Liang, Z. Chen, L. Xu, J. Wang, J. Yin, G.-A. Yu, Z.-N. Chen and S. H. Liu, *J. Mater. Chem. C*, 2014, ***2***, 2243−2250.

5 Interesting materials combining Au^{III} and Ag^{I} centres and showing hort Ag···Ag interactions have been reported very recently: J. Fernandez-Cestau, R. J. Rama, L. Rocchigiani, B. Bertrand, E. Lalinde, M. Linnolahti, M. Bochmann, *Inorg. Chem.*, 2019, ***58***, 2020−2030.

6 For Au^{I}/Ag^{I} bimetallic compounds with direct Au···Ag interactions see: (a) T. Lasanta, M. E. Olmos, A. Laguna, J. M. López-de-Luzuriaga and P. Naumov, *J. Am. Chem. Soc*., 2011, ***133***, 16358–16361. (b) W.-X. Ni, Y.-M. Qiu, M. Li, J. Zheng, R. W.-Y. Sun, S.-Z. Zhan, S. W. Ng and D. Li, *J. Am. Chem. Soc*., 2014, ***136***, 9532–9535. (c) R. Donamaría, V. Lippolis, J. M. López-de-Luzuriaga, M. Monge, M. Nieddu and M. E. Olmos, *Inorg. Chem*., 2018, ***57***, 11099−11112.

7 E. J. Fernández, A. Laguna, J. M. López-de-Luzuriaga, M. Monge, M. Montiel and M. E. Olmos, *Inorg. Chem*., 2005, ***44***, 1163–1165.

8 As reported previously for compound **1** and others: C. Bartolomé, M. Carrasco-Rando, S. Coco, C. Cordovilla, P. Espinet and J. M. Martin-Alvarez, *Dalton Trans*., 2007, 5339–5345.

9 Probably the record of identified polymorphism is a dozen of X-Ray structures of different polymorphs of the same compound: T. Seki, M. Jin and H. Ito, *Inorg. Chem*., 2016, ***55***, 12309–12320.

10 J. E. Huheey, Inorganic Chemistry SI Units Edition, 1st edition, p. 184. Harper & Row, 1975.

11 Short halogen-halogen interactions in crystal structures have been reported before: (a) R. Bayón, S. Coco and P. Espinet, *Chem. – Eur. J*., 2005, ***11***, 1079–1085. (b) S. K. Nayak, M. K. Reddy, T. N. G. Row and D. Chopra, *Cryst. Growth Des*., 2011, ***11***, 1578–1596. (c) T. Seki, K. Ida and H. Ito, *Mater. Chem. Front*., 2018, ***2***, 1195–1200.

12 A distance of 3.03 Å for the halogen-halogen $F_3C–Cl^{\delta+}\cdots\ ^{\delta-}F–CH_3$ interaction was theoretically predicted: D. Hauchecorne and W. A. Herrebout, *J. Phys. Chem. A*, 2013, ***117***, 11548–11557.

13 The shortest Au···Au distances due to aurophilicity are about 3.0 Å: H. Schmidbaur and A. Schier, *Chem. Soc. Rev*., 2008, ***37***, 1931–1951.

14 T. Seki, K. Kobayashi, T. Mashimo and H. Ito, *Chem. Commun*., 2018, ***54***, 11136–11139.

15 The lifetimes are borderline between fluorescence and phosphorescence: M. A. Omary and H. H. Patterson in Luminescence, Theory, Encyclopedia of spectroscopy and spectrometry, vol. 2, pp. 1186–1207. Elsevier, Ltd. 1999.

16 T. Seki, N. Tokodai, S. Omagari, T. Nakanishi, Y. Hasegawa, T. Iwasa, T. Taketsugu and H. Ito, *J. Am. Chem. Soc*., 2017, ***139***, 6514–6517.

17 In our case the luminescence switch is provoked by a crystal-to-amorphous transition. There are a few studies of mechanically stimulated crystal-to-crystal transitions. In all cases shorter Au···Au distances lead to higher red-shifts of the emission: (a) H. Ito, M. Muromoto, S. Kurenuma, S. Ishizaka, N. Kitamura, H. Sato and T. Seki, *Nat. Commun*., 2013, ***4***, 2009–2013. (b) T. Seki, K. Sakurada and H. Ito, *Angew. Chem. Int. Ed*., 2013, ***52***, 12828–12832.

18 (a) M. Jin, T. Sumitani, H. Sato, T. Seki and H. Ito, *J. Am. Chem. Soc*., 2018, ***140***, 2875–2879. (b) M. Jin, T. Seki and H. Ito, *Chem. Commun*., 2016, ***52***, 8083–8086.

19 HOMO (2), LUMO (2) and LUMO (4) represent in fact a groups of several orbital combinations very close in energy, whereas σ*-HOMO (4) is an individual orbital.

20 A detailed study using QM/MM calculations has been published recently: S. Aono, T. Seki, H. Ito and S. Sakaki, J. Phys. Chem. C, 2019, ***123***, 4773–4794.